Mironov and Mironov
Advances in Aerodynamics (2024) 6:8
https://doi.org/10.1186/s42774-023-00171-z

Advances in Aerodynamics

RESEARCH

Open Access

Vortex model of plane turbulent air flows in channels

Victor L. Mironov[1*] and Sergey V. Mironov[1]

*Correspondence: mironov@ipmras.ru

[1] Institute for Physics of Microstructures RAS, Nizhny Novgorod 603950, Russia

Abstract

We present a theoretical model of plane turbulent flows based on the previously proposed equations, which take into account both the longitudinal motion and the vortex tube rotation. Using the simple model of eddy viscosity, we obtain the analytical expressions for the mean velocity profiles of stationary turbulent flows. In particular, we consider the near-wall flow over a flat plate in a wind tunnel as well as Couette and Poiseuille flows in rectangular channels. In all these cases, the calculated velocity profiles are in good agreement with experimental data and results of direct numerical simulations.

Keywords: Vortex model of turbulence, Eddy viscosity, Plane wall-bounded flows, Couette flow, Poiseuille flow

1 Introduction

The plane near-wall (boundary layer) flows [1–3] and wall-bounded Couette [4–10] and Poiseuille [11–14] flows are actively investigated both theoretically and experimentally for a long time. These are relatively simple shear flows of air and fluid, which are realized in rectangular channels and often used as model flows to test various theoretical models. The theoretical description of turbulent flows is based on the solution of the Reynolds-averaged Navier–Stokes (RANS) equation with the Reynolds stress tensor, which takes into account the influence of the fluctuating part of the velocity on the average flow characteristics [15, 16]. However, calculating the Reynolds tensor is a difficult problem. One of the basic ideas is that turbulent (eddy) viscosity depends on the coordinates in the flow, which make it possible to reconcile the theoretical calculations with experimental data by using various models of boundary layer [17–20]. The main progress in the theoretical description of turbulence is associated with the development of two-equation models [21, 22] such as $k-\varepsilon$ model [23–25] and $k-\omega$ model [26, 27]. The advantages and disadvantages of various models are considered in [28, 29]. With the development of computer technologies, the methods for the direct numerical simulations (DNS) have become widespread. The DNS methods allow one to simulate the evolution of steady and unsteady flows and calculate the average values of various flow characteristics [30–34].

The turbulent flow is characterized by vortex movements with a wide range of spatial scales. However, existing analytical models of turbulence [35–38] are based on various models of the Reynolds stress tensor, but do not explicitly take into account the vortex structure of the turbulent flow. In the present paper, we develop a model in which the vortex tubes are directly involved in the formation of turbulent wall-bounded flows. We describe a turbulent flow based on the symmetric Maxwell-like system of equations explicitly accounting vortex motion. In the literature, there are a number of works, in which Maxwell-type equations for the velocity and the vorticity vectors are used to describe the vortex flow [39–41]. In particular, these equations are applied for the consideration of turbulent flows [40] and electron–ion plasma [42]. However, in these papers, the additional equation for vorticity is actually obtained by applying the "curl" operator to the Euler equation, so the resulting equation is not independent. We developed a different approach based on Helmholtz droplet model of a fluid [43] and obtained alternative Maxwell-type equations, which take into account the longitudinal motion and rotation of vortex tubes [44]. These equations were used in the hydrodynamic model of electron–ion plasma [45] and in the model of electron fluid in solids [46]. In the present paper, we apply this approach for the description of plane near-wall turbulent flows in wind tunnels as well as for Couette and Poiseuille flows in rectangular channels.

2 Symmetric equations of droplet model of vortex flow

In this section we briefly recall the main provisions of the droplet model of vortex fluid and the qualitative derivation of the main equations. The flow of non-viscous fluid is described by the system of equations [47] including the Euler equation and the continuity equation:

$$\begin{aligned} &\frac{\partial \boldsymbol{v}}{\partial t}+(\boldsymbol{v}\cdot\nabla)\boldsymbol{v}+\frac{1}{\rho}\nabla p=0,\\ &\frac{\partial \rho}{\partial t}+(\boldsymbol{v}\cdot\nabla)\rho+\rho(\nabla\cdot\boldsymbol{v})=0. \end{aligned} \tag{1}$$

This system can be rewritten in a symmetric form. We will consider the flow under the condition of constant entropy $s(\boldsymbol{r},t)=const$ (s is the entropy per unit mass). Let us use the thermodynamic relation for enthalpy (ε):

$$d\varepsilon = Tds+\frac{1}{\rho}dp. \tag{2}$$

Then, introducing a new function $u=\frac{1}{c}\varepsilon$, we find that the following relations hold:

$$du=\frac{1}{c}d\varepsilon=\frac{1}{c\rho}dp=\frac{c}{\rho}d\rho. \tag{3}$$

Here c is the speed of sound $\left(c^2=(\partial p/\partial\rho)_s=const\right)$. Accordingly, all values in Eqs. (1) can be expressed through the function u,

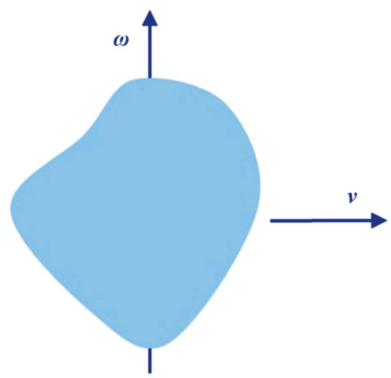

Fig. 1 Sketch of a fluid particle moving with speed ***v*** and rotating with angular speed ***ω*** around an instantaneous axis

$$\begin{aligned} &\frac{1}{\rho}\nabla p = c\nabla u, \\ &\frac{\partial \rho}{\partial t} = \frac{\rho}{c}\frac{\partial u}{\partial t}, \\ &\nabla \rho = \frac{\rho}{c}\nabla u. \end{aligned} \tag{4}$$

Substituting (4) into (1) we obtain the following symmetric system of equations:

$$\begin{aligned} &\frac{1}{c}\left(\frac{\partial}{\partial t} + (\boldsymbol{v}\cdot\nabla)\right)\boldsymbol{v} + \nabla u = 0, \\ &\frac{1}{c}\left(\frac{\partial}{\partial t} + (\boldsymbol{v}\cdot\nabla)\right)u + \nabla\cdot\boldsymbol{v} = 0. \end{aligned} \tag{5}$$

To describe vortex flows, Helmholtz [43] proposed a drop model of fluid. According to this model, the change that an arbitrary infinitesimal particle of fluid (Fig. 1) undergoes during infinitesimal time consists of three different motions: 1) a transition of the particle through space; 2) an expansion or contraction of the particle parallel to three main axes of dilatation so that every rectangular parallelepiped in water, whose edges are parallel to the main directions of dilatation remains rectangular; 3) a rotation around a temporary axis of rotation. During rotation, the particle is considered to instantly solidify and the angular velocity of its rotation $\boldsymbol{\omega}$ is related to the linear velocity $\boldsymbol{v}$ inside the drop by the following relation:

$$2\boldsymbol{\omega} = \nabla\times\boldsymbol{v}. \tag{6}$$

Since angular velocity $\boldsymbol{\omega}$ is the derivative of the vector of rotation angle $\boldsymbol{\theta}$,

$$\boldsymbol{\omega} = \frac{d\boldsymbol{\theta}}{dt}, \tag{7}$$

we will describe the vortex flow using the field $\boldsymbol{\theta}(\boldsymbol{r}, t)$. Vortex lines are the lines whose direction coincides with the direction of the instantaneous axis of rotation of the fluid particles. In turn, particles located along the vortex lines form vortex filaments, the combination of which forms the vortex tubes [48].

Taking into account (6) and (7), the vortex tube rotation is described by the following equation:

$$\left(\frac{\partial}{\partial t} + (\boldsymbol{v}\cdot\nabla)\right)\boldsymbol{\theta} - \nabla\times\boldsymbol{v} = 0. \tag{8}$$

In order to give this equation a symmetric form similar to Eqs. (5), we introduce a new function $\boldsymbol{w} = c\,\boldsymbol{\theta}$ and then we obtain

$$\frac{1}{c}\left(\frac{\partial}{\partial t} + (\boldsymbol{v}\cdot\nabla)\right)\boldsymbol{w} - \nabla\times\boldsymbol{v} = 0. \tag{9}$$

The condition

$$\nabla\cdot\boldsymbol{w} = 0 \tag{10}$$

describes the vortex tube without twisting. To take into consideration the twisting effect, this equation is modified as follows:

$$\frac{1}{c}\left(\frac{\partial}{\partial t} + (\boldsymbol{v}\cdot\nabla)\right)\xi + \nabla\cdot\boldsymbol{w} = 0, \tag{11}$$

where the function ξ is proportional to the twist angle [44].

Taking into account Eqs. (5), (9) and (11), the symmetric system of equations for vortex flow can be represented in the following form:

$$\begin{aligned}
&\frac{1}{c}\left(\frac{\partial}{\partial t} + (\boldsymbol{v}\cdot\nabla)\right)\boldsymbol{v} + \nabla\times\boldsymbol{w} + \nabla u = 0,\\
&\frac{1}{c}\left(\frac{\partial}{\partial t} + (\boldsymbol{v}\cdot\nabla)\right)u + \nabla\cdot\boldsymbol{v} = 0,\\
&\frac{1}{c}\left(\frac{\partial}{\partial t} + (\boldsymbol{v}\cdot\nabla)\right)\boldsymbol{w} - \nabla\times\boldsymbol{v} + \nabla\xi = 0,\\
&\frac{1}{c}\left(\frac{\partial}{\partial t} + (\boldsymbol{v}\cdot\nabla)\right)\xi + \nabla\cdot\boldsymbol{w} = 0.
\end{aligned} \tag{12}$$

To describe the viscous fluid, it is necessary to make the following replacement of operators in all equations:

$$\frac{1}{c}\left(\frac{\partial}{\partial t} + (\boldsymbol{v}\cdot\nabla)\right) \Rightarrow \frac{1}{c}\left(\frac{\partial}{\partial t} + (\boldsymbol{v}\cdot\nabla) - \nu\Delta\right), \tag{13}$$

where ν is the kinematic viscosity. Thus finally we have the following symmetric system of equations:

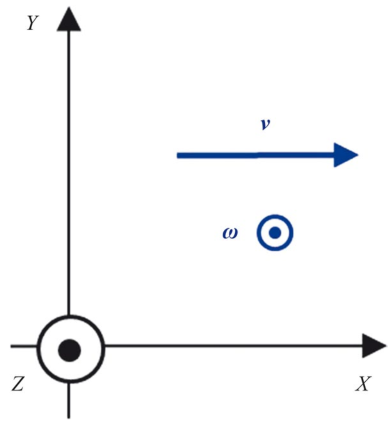

Fig. 2 Sketch of the coordinate system for the plane flow

$$\begin{aligned}
&\frac{1}{c}\left(\frac{\partial}{\partial t}+(\boldsymbol{v}\cdot\nabla)-\nu\Delta\right)\boldsymbol{v}+\nabla\times\boldsymbol{w}+\nabla u=0,\\
&\frac{1}{c}\left(\frac{\partial}{\partial t}+(\boldsymbol{v}\cdot\nabla)-\nu\Delta\right)u+\nabla\cdot\boldsymbol{v}=0,\\
&\frac{1}{c}\left(\frac{\partial}{\partial t}+(\boldsymbol{v}\cdot\nabla)-\nu\Delta\right)\boldsymbol{w}-\nabla\times\boldsymbol{v}+\nabla\xi=0,\\
&\frac{1}{c}\left(\frac{\partial}{\partial t}+(\boldsymbol{v}\cdot\nabla)-\nu\Delta\right)\xi+\nabla\cdot\boldsymbol{w}=0.
\end{aligned} \tag{14}$$

A rigorous sequential method for deriving Eqs. (14) is based on the use of space-time Clifford algebra and is described in detail in [44].

3 Vortex model of plane turbulent flow

Let us consider the plane flow parallel to the plane xy with the velocity directed along the X axis (Fig. 2).

In this case the velocity $\boldsymbol{v}$ has only x component and depends only on y coordinate $v_x = v_x(y,t)$. Similarly, in plane flow the vector $\boldsymbol{w}$ has only z component and depends only on y coordinate $w_z = w_z(y,t)$. Since we assume the uniform flow distribution in the Z direction and no torques, the vortex tubes have no twisting $\xi = 0$. Also we suppose that enthalpy depends only on x coordinate $u = u(x,t)$ and the gradient of enthalpy to be constant,

$$\frac{\partial u}{\partial x}=\frac{1}{c\rho}\frac{\partial p}{\partial x}=-g. \tag{15}$$

Then in the projection on the X and Z axes, the system (14) takes the following form:

$$\begin{aligned}
&\frac{1}{c}\frac{\partial v_x}{\partial t}-\frac{\nu}{c}\frac{\partial^2 v_x}{\partial y^2}+\frac{\partial w_z}{\partial y}-g=0,\\
&\frac{1}{c}\frac{\partial w_z}{\partial t}-\frac{\nu}{c}\frac{\partial^2 w_z}{\partial y^2}+\frac{\partial v_x}{\partial y}=0.
\end{aligned} \tag{16}$$

To describe a steady-state turbulent flow, we introduce the time-averaged values. For any value $a(y,t)$, averaging over time is carried out as follows:

$$\bar{a}(y) = \lim_{T\to\infty} \frac{1}{2T} \int_{-T}^{T} a(y,t)\,dt. \tag{17}$$

Then the local velocity and vector of rotation can be represented as

$$\begin{aligned} &\boldsymbol{v}(\boldsymbol{r},t) = \overline{\boldsymbol{v}}(\boldsymbol{r}) + \boldsymbol{v}'(\boldsymbol{r},t),\\ &\boldsymbol{w}(\boldsymbol{r},t) = \overline{\boldsymbol{w}}(\boldsymbol{r}) + \boldsymbol{w}'(\boldsymbol{r},t), \end{aligned} \tag{18}$$

where $\boldsymbol{v}'$ and $\boldsymbol{w}'$ are corresponding fluctuations. For components we have

$$\begin{aligned} &v_x(y,t) = \overline{v}_x(y) + v_x'(y,t),\\ &w_z(y,t) = \overline{w}_z(y) + w_z'(y,t). \end{aligned} \tag{19}$$

In function $w_z(y,t)$ we separate the part associated with the regular rotation of the vortex tubes with angle velocity $\omega_z(y)$ and the part associated with irregular rotation $\varphi_z(y,t)$,

$$w_z(y,t) = 2c\omega_z(y)t + \varphi_z(y,t). \tag{20}$$

Following (17) and (20), for a stationary flow we have

$$\begin{aligned} &\overline{\frac{\partial v_x}{\partial t}} = 0,\\ &w_z'(y,t) = \varphi_z'(y,t),\\ &\overline{w}_z(y) = \overline{\varphi}_z(y),\\ &\overline{\frac{\partial w_z}{\partial t}} = 2c\omega_z(y). \end{aligned} \tag{21}$$

Substituting (18) into Eqs. (14) and averaging over time we obtain (taking into account (20) and (21)) the following time-averaged plane flow equations:

$$\begin{aligned} &-\frac{\nu}{c}\frac{\partial^2\overline{v}_x}{\partial y^2} + \frac{1}{c}\frac{\partial}{\partial y}\overline{v_x'v_y'} + \frac{\partial\overline{\varphi}_z}{\partial y} - g = 0,\\ &-\frac{\nu}{c}\frac{\partial^2\overline{\varphi}_z}{\partial y^2} + \frac{1}{c}\frac{\partial}{\partial y}\overline{\varphi_z'v_y'} + \frac{\partial\overline{v}_x}{\partial y} + 2\omega_z(y) = 0. \end{aligned} \tag{22}$$

Here $\overline{v_x'\,v_y'}$ and $\overline{\varphi_z'v_y'}$ are the components of the corresponding Reynolds stress tensors. Following to the Boussinesq assumption [49, 50], we suppose that components of stress tensors can be written as

$$-\overline{v_x'v_y'} = \nu_T\frac{\partial\overline{v}_x}{\partial y}, \tag{23}$$

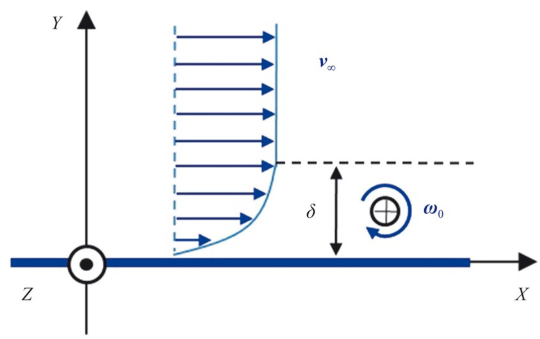

Fig. 3 Sketch of a stationary turbulent flow over an infinite plate. The vortex tubes in the thin layer, on average, rotate with angular velocity $\boldsymbol{\omega}_0$

$$-\overline{\varphi_z' v_y'} = \nu_T \frac{\partial \overline{\varphi}_z}{\partial y}, \tag{24}$$

where ν_T is the turbulent kinematic viscosity. We will suppose that $\nu_T = const$, then we obtain a very simple model of turbulent flow, which is described by the following equations:

$$\begin{aligned} &-\lambda \frac{\partial^2 \overline{v}_x}{\partial y^2} + \frac{\partial \overline{\varphi}_z}{\partial y} - g = 0, \\ &-\lambda \frac{\partial^2 \overline{\varphi}_z}{\partial y^2} + \frac{\partial \overline{v}_x}{\partial y} + 2\omega_z(y) = 0. \end{aligned} \tag{25}$$

Here we introduce the turbulent length $\lambda = \dfrac{\nu + \nu_T}{c}$.

In the next sections, we will explore how this simple model describes the different plane turbulent wall-bounded flows.

4 Model of turbulent flow in near-wall layer

Let us consider a simple model of steady-state turbulent flow over an infinite plate (Fig. 3). We believe that shear flow exists only in a thin near-wall layer of thickness δ. The velocity outside the boundary layer is v_∞ and the pressure gradient is zero ($g = 0$). Also we assume that on average all vortex tubes in the near-wall layer rotate with the same angular velocity $\omega_z(y) = -\omega_0$. In this case Eqs. (25) take the following form:

$$\begin{aligned} &-\lambda \frac{\partial^2 \overline{v}_x}{\partial y^2} + \frac{\partial \overline{\varphi}_z}{\partial y} = 0, \\ &-\lambda \frac{\partial^2 \overline{\varphi}_z}{\partial y^2} + \frac{\partial \overline{v}_x}{\partial y} - 2\omega_0 = 0. \end{aligned} \tag{26}$$

We choose the boundary conditions corresponding to the complete adhesion to the plate surface:

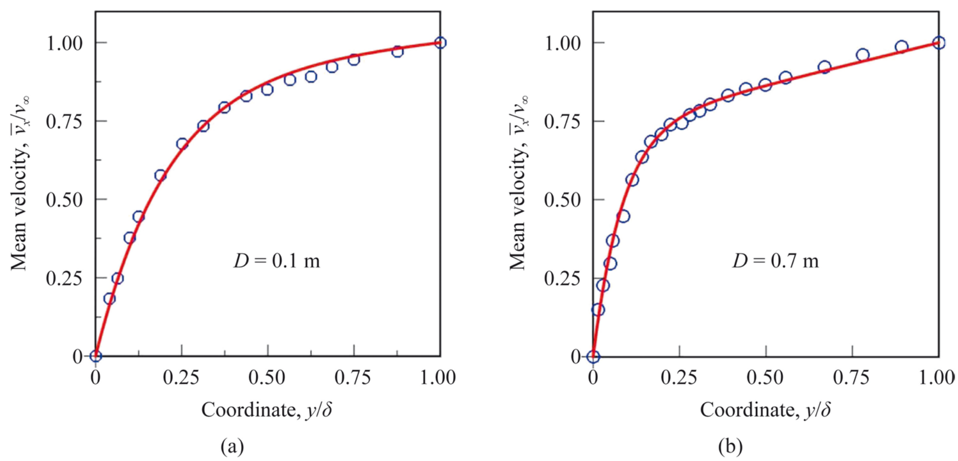

Fig. 4 Velocity profiles over the plate at different distances (*D*) from the leading edge. Circles (◯) are the experimental data [1]; solid red lines correspond to the distribution (28). Fitting parameters are **a** $\lambda/\delta = 0.21,\ \beta = 0.1$; **b** $\lambda/\delta = 0.085, \beta = 0.27$

$$\begin{aligned} &\overline{v}_x(0) = 0, \\ &\overline{v}_x(\delta) = v_\infty, \\ &\overline{\varphi}_z(0) = 0, \\ &\overline{\varphi}_z(\delta) = \varphi_\delta. \end{aligned} \tag{27}$$

The solution of system (26) in the region $0 \leq y \leq \delta$ has the following form:

$$\overline{v}_x = v_\infty \left\{ (1-\beta)\frac{1-\exp\left(-y/\lambda\right)}{1-\exp(-\delta/\lambda)} + \beta y/\delta \right\}, \tag{28}$$

$$\overline{\varphi}_z = \varphi_0 \frac{1-\exp\left(-y/\lambda\right)}{1-\exp(-\delta/\lambda)}. \tag{29}$$

Here we introduce the dimensionless parameter $\beta = 2\omega_0\delta/v_\infty$. The values φ_δ and v_∞ are related by the following relation:

$$\varphi_\delta = -v_\infty(1-\beta). \tag{30}$$

As an example, we consider the approximation of experimental data on plate blowing in a wind tunnel (Gete & Evans [1]) using formula (28). Figure 4 demonstrates the fitting of the experimental velocity profiles in the boundary layer at distances of 0.1 m and 0.7 m from the leading edge of the plate. In both cases, there is good agreement between the fitting curves and the experimental data. A comparison of the fitting parameters shows that with increasing distance from the edge, the turbulent viscosity decreases (parameter λ/δ), while the angular velocity of rotation of the vortex tubes (parameter β) increases.

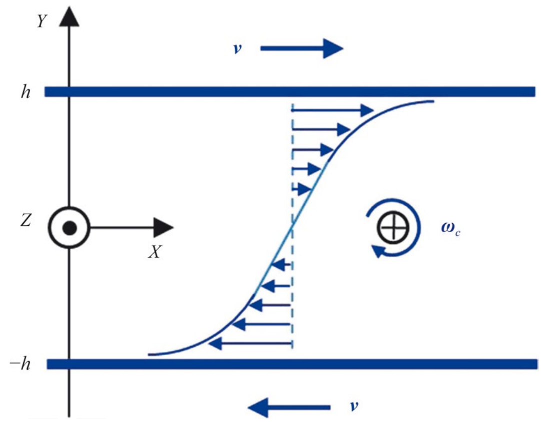

Fig. 5 Sketch of a plane Couette flow between two infinite plates, which move along the *X* axis with speed *v* in opposite directions

5 Turbulent Couette flow

Let us consider a turbulent flow formed between two infinite parallel plates moving relative to each other in opposite directions (Fig. 5).

Let us consider a fully developed turbulent flow, in which the vortex tubes on average rotate with a constant angular velocity $\omega_z(y) = -\omega_c$. Then Eqs. (25) take the following form:

$$\begin{aligned} &-\lambda\frac{\partial^2\overline{v}_x}{\partial y^2}+\frac{\partial\overline{\varphi}_z}{\partial y}=0,\\ &-\lambda\frac{\partial^2\overline{\varphi}_z}{\partial y^2}+\frac{\partial\overline{v}_x}{\partial y}-2\omega_c=0. \end{aligned} \tag{31}$$

As the boundary conditions, we choose

$$\begin{aligned} &\overline{v}_x(h)=v,\\ &\overline{v}_x(-h)=-v,\\ &\overline{\varphi}_z(h)=0,\\ &\overline{\varphi}_z(-h)=0. \end{aligned} \tag{32}$$

The solutions of Eqs. (31) are written as

$$\overline{v}_x=v\left\{\alpha\frac{y}{h}+(1-\alpha)\frac{\sinh(y/\lambda)}{\sinh(h/\lambda)}\right\}, \tag{33}$$

$$\overline{\varphi}_z=(1-\alpha)v\frac{\cosh(y/\lambda)-\cosh(h/\lambda)}{\sinh(h/\lambda)}. \tag{34}$$

Here we introduce the dimensionless parameter,

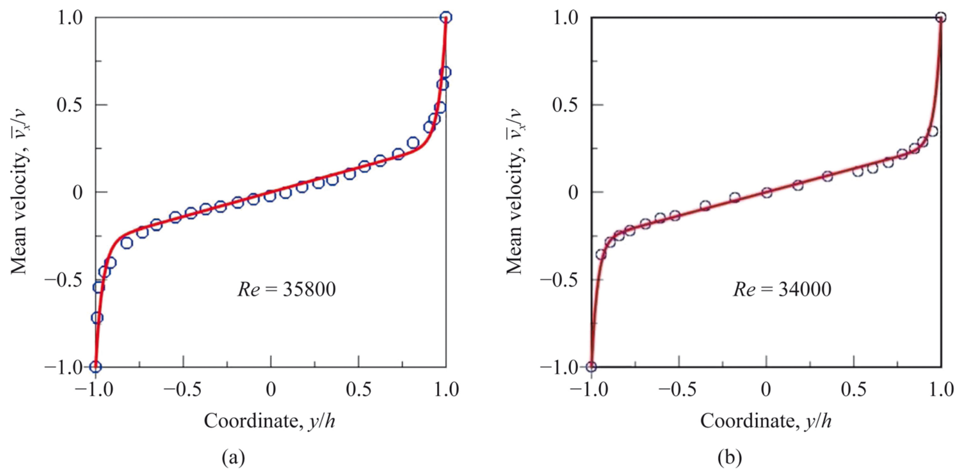

Fig. 6 Distributions of the mean velocity in a turbulent Couette flow. Circles (◯) are the experimental results [5, 13]; solid red lines correspond to (33). Fitting parameters are **a** $\lambda/h = 0.04$, $\alpha = 0.28$; **b** $\lambda/h = 0.035$, $\alpha = 0.27$

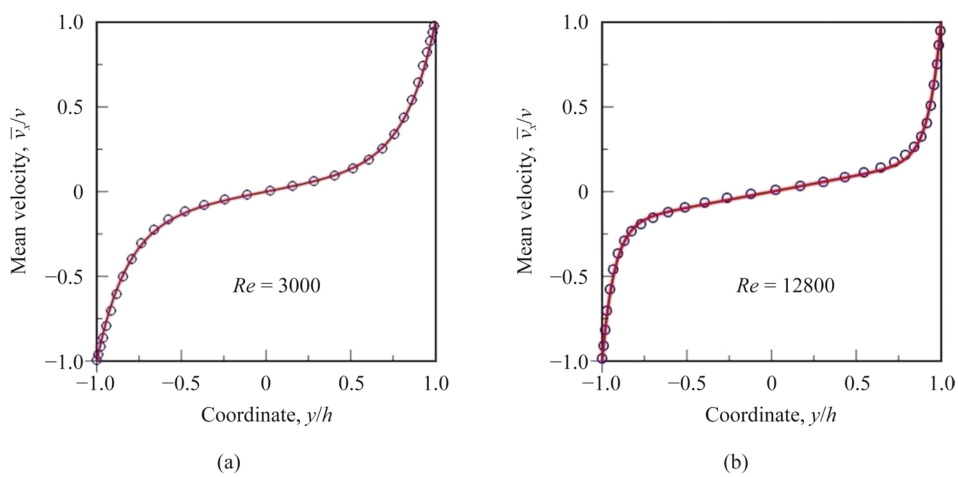

Fig. 7 DNS profiles of the mean velocity in a turbulent Couette flow. **a** Circles (◯) are the results of DNS with $Re = 3000$ [51]; the solid red line corresponds to (33) at $\lambda/h = 0.16$, $\alpha = 0.21$. **b** Circles (◯) are the DNS results with $Re = 12800$ [52]; the solid red line corresponds to (33) at $\lambda/h = 0.072$, $\alpha = 0.189$

$$\alpha = \frac{2\omega_c h}{\nu}. \tag{35}$$

As an example, we consider the approximation of experimental velocity profiles by the normalized distribution (33). Figure 6 shows the comparison of the mean velocity profiles for air (El Telbany & Reynolds [13]) and water (Reichardt [5]) flows at close Reynolds numbers (*Re*). As can be seen, distribution (33) is in good agreement with experimental data. The fitting parameters λ/h, and α in these two cases are also very close. In addition, Fig. 7 demonstrates the comparison of solution (33) with the DNS results for Couette flow with $Re = 3000$ (Tsukahara et al. [51]) and $Re = 12800$ (Kawamura et al. [52]). In both cases, the fitted profiles are in good agreement with the results of the DNS. Here we also observe a decrease of turbulent viscosity (parameter λ/h) and an increase of angular velocity ω_c (parameter α) with increasing *Re*.

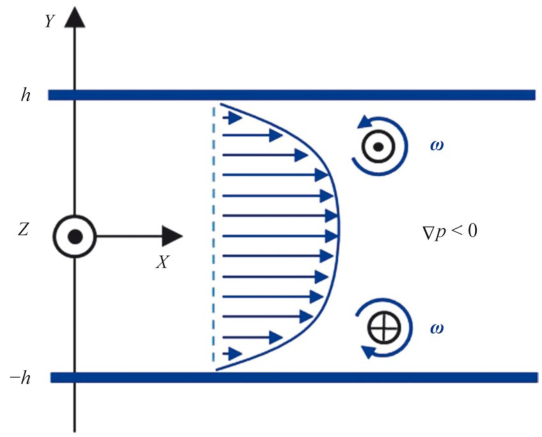

Fig. 8 Sketch of a plane turbulent Poiseuille flow in a channel between two infinite plates

6 Turbulent Poiseuille flow

In case of plane Poiseuille flow in a channel with fixed walls (Fig. 8), the air moves under the action of a pressure gradient.

Let us consider a fully developed turbulent Poiseuille flow taking into account the vortex tube rotation. We assume that the angle velocity of vortex tube rotation is a linear function of y coordinate $\omega_z(y) = \kappa y$. In this case Eqs. (25) take the following form:

$$\begin{aligned} -\lambda\frac{\partial^2\overline{v}_x}{\partial y^2} + \frac{\partial\overline{\varphi}_z}{\partial y} - g = 0, \\ -\lambda\frac{\partial^2\overline{\varphi}_z}{\partial y^2} + \frac{\partial\overline{v}_x}{\partial y} + 2\kappa y = 0, \end{aligned} \tag{36}$$

with the following boundary conditions:

$$\begin{aligned} \overline{v}_x(h) = \overline{v}_x(-h) = 0, \\ \overline{\varphi}_z(h) = \overline{\varphi}_z(-h) = 0. \end{aligned} \tag{37}$$

The solutions of system (36) are

$$\overline{v}_x = \sigma gh\frac{\cosh(h/\lambda) - \cosh(y/\lambda)}{\sinh(h/\lambda)} + gh^2\frac{(1-\sigma)}{2\lambda}\left(1 - \frac{y^2}{h^2}\right), \tag{38}$$

$$\overline{\varphi}_z = -\sigma gh\frac{\sinh(y/\lambda)}{\sinh(h/\lambda)} + \sigma gy. \tag{39}$$

Here σ is a certain dimensionless parameter connected with pressure gradient and transverse gradient of angular velocity,

$$\sigma = 1 - \frac{2\lambda\kappa}{g}. \tag{40}$$

This parameter describes the relationship between the parabolic and hyperbolic velocity profiles. At $\sigma = 0$, the profile is purely parabolic, and at $\sigma = 1$, it is hyperbolic.

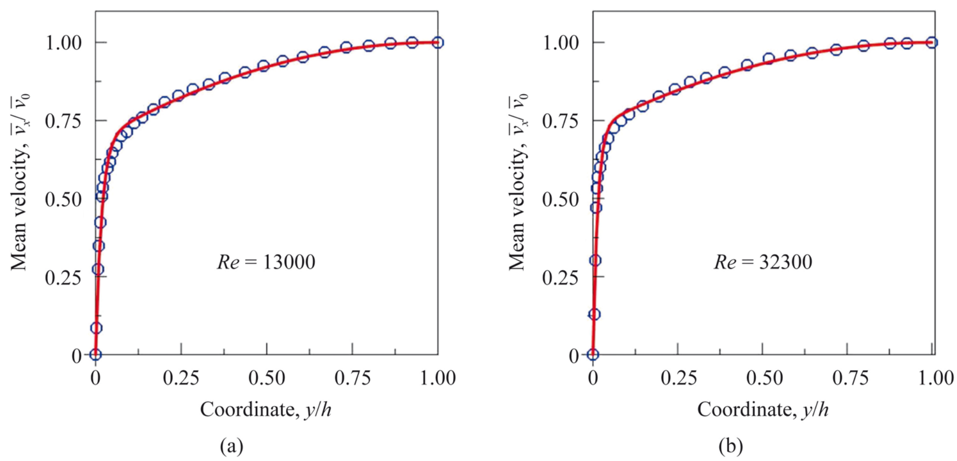

Fig. 9 The profiles of mean velocity for plane Poiseuille flow at different *Re*. Experimental data are shown by circles [12]. The profiles corresponding to formula (38) are shown by solid red lines. **a** $\lambda/h = 0.0178$, $\sigma = 0.984$; **b** $\lambda/h = 0.014$, $\sigma = 0.9896$

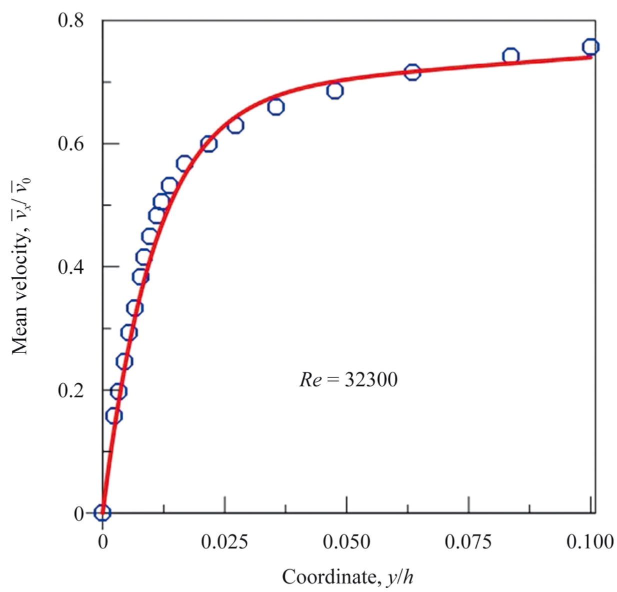

Fig. 10 The profiles of mean velocity near the wall. Experimental data [12] are shown by circles; the solid red line corresponds to formula (38). Fitting parameters are $\lambda/h = 0.0107$, $\sigma = 0.99$

As an example, we consider the approximation of experimental data for air flows in rectangular channels by the normalized distribution (38). The normalization is $\overline{v}_x/\overline{v}_0$ (where $\overline{v}_0$ is the velocity at $y = 0$). Figure 9 shows the fitting of the experimental mean velocity profiles (Hussain & Reynolds [12]) for different *Re*. As can be seen from the comparison of the fitting parameters, an increase in *Re* is accompanied by a decrease in turbulent viscosity (parameter λ/h) and an increase in parameter σ. In addition, Fig. 10 demonstrates a more accurate match between the calculated velocity distribution and the experimental profile (Hussain & Reynolds [12]) in the region near a wall. Figure 11 shows the results of comparing mean velocity profiles calculated using formula (38) and DNS data for $Re = 2013$ (Tsukahara [53]) and $Re = 24428$ (Kawamura

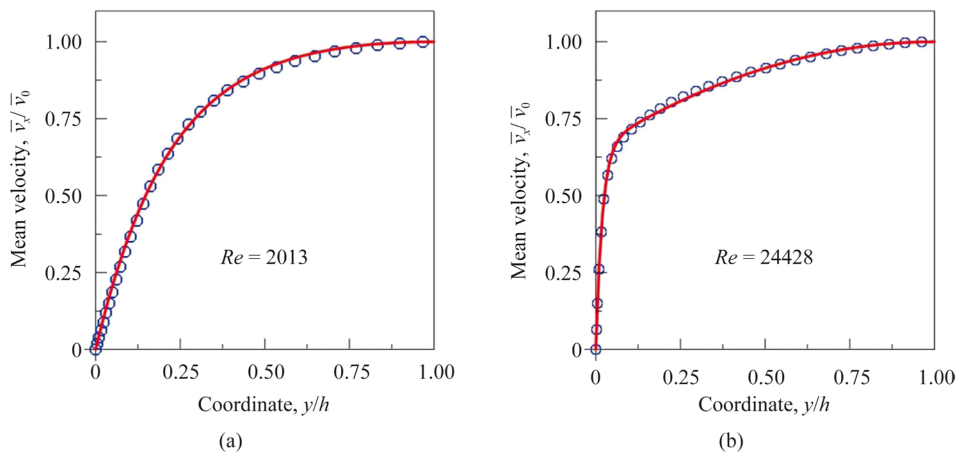

Fig. 11 The mean velocity profiles of a turbulent Poiseuille flow. DNS data [53, 54] are shown by circles; the solid red line corresponds to the simulated profile (38). The fitting parameters are **a** $\lambda/h = 0.21$, $\sigma = 0.975$; **b** $\lambda/h = 0.019$, $\sigma = 0.981$

et al. [54]). In all considered cases, there is good agreement of calculated velocity profiles with experimental results and DNS data.

7 Discussion

The proposed vortex model of turbulent flow differs from the generally accepted approach. In this model, for a plane turbulent flow we have two Eqs. (25) describing the longitudinal motion and rotation of the vortex tubes. On the other hand, in the RANS model we have only one equation, which for the plane Poiseuille flow has the following form:

$$-\frac{\nu}{c}\frac{\partial^2 \overline{v}_x}{\partial y^2} + \frac{1}{c}\frac{\partial}{\partial y}\overline{v'_x v'_y} - g = 0. \tag{41}$$

In this case, the Boussinesq hypothesis (23) with a constant eddy viscosity does not describe the change in the velocity profile of a turbulent flow. The profile remains parabolic. Therefore, to obtain satisfactory agreement with experimental data within the framework of the RANS equation, it is generally accepted that the eddy viscosity depends on the coordinates $\nu_T = \nu_T(y)$. It leads us to the following equation:

$$\nu\frac{\partial^2 \overline{v}_x}{\partial y^2} + \frac{\partial}{\partial y}\left(\nu_T(y)\frac{\partial \overline{v}_x}{\partial y}\right) - cg = 0, \tag{42}$$

and the main issue is the choice of the model of the eddy viscosity profile $\nu_T(y)$. The analytical expression for the eddy viscosity was suggested by Cess [55]. According to Cess's model, the eddy viscosity profile can be represented in the following form [56]:

$$\nu_T(\eta) = \frac{\nu}{2}\left\{1 + \frac{K^2 Re_\tau^2}{9}\left(1-\eta^2\right)^2\left(1+2\eta^2\right)^2\left(1 - \exp\left[(|\eta|-1)\frac{Re_\tau}{A}\right]\right)^2\right\}^{1/2} + \frac{\nu}{2}, \tag{43}$$

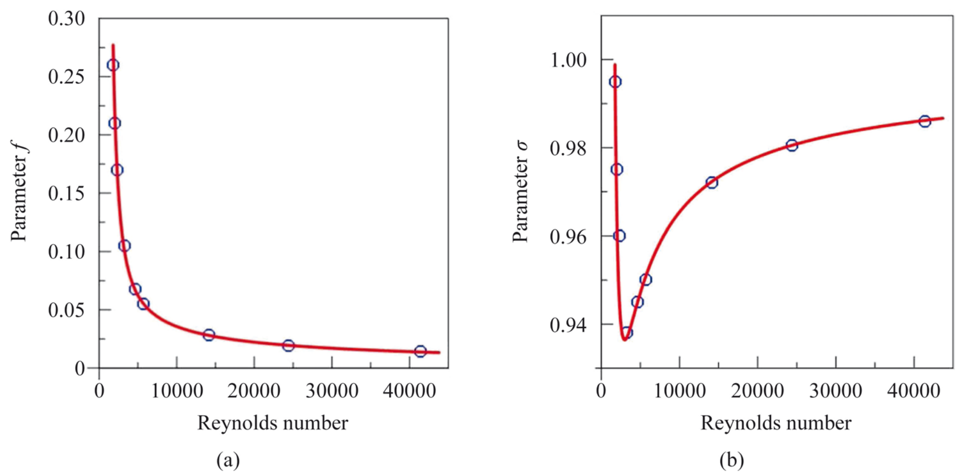

Fig. 12 Dependencies of parameters **a** f and **b** σ on Reynolds number. Circles are the data obtained from fitting of DNS velocity profiles [58] (see Table 1); solid lines correspond to the power-law approximations (47) and (48)

where $\eta = y/h$ is the normalized coordinate across the channel, Re_τ is the friction Reynolds number, K is the von Karman constant of logarithmic velocity profile, and A is the constant in van Driest's wall law [57]. The mean velocity profile can be found from (42) as

$$\overline{v}_x(\eta) = cg \int_{-1}^{\eta} \frac{\eta + 1}{\nu + \nu_T(\eta)} d\eta, \tag{44}$$

where the integral can be calculated by the appropriate numerical method.

In the proposed vortex model, the turbulent flow is described by two equations, and the Boussinesq hypothesis (23) with constant eddy viscosity $\nu_T = const$ immediately gives us the combined hyperbolic-parabolic mean velocity profile (38) in analytical form. The distribution of mean velocity is defined by two parameters $f = \lambda/h$ and σ (40). Eddy viscosity can be estimated using parameter f as

$$\nu_T = chf(Re) - \nu. \tag{45}$$

In addition, the gradient of angular velocity κ can be estimated as

$$\kappa = \frac{1 - g\,\sigma(Re)}{2hf(Re)}. \tag{46}$$

The dependencies of $f(Re)$ and $\sigma(Re)$ can be extracted from experimental data or from results of DNS. As an example, Fig. 12 shows the dependencies of parameters f and σ on the Reynolds number for the Poiseuille flow, obtained from fitting velocity

Table 1 The values of the fitting parameters f and σ

Re	1844	2013	2293	3285	4653	5731	14147	24428	41441
f	0.26	0.21	0.17	0.105	0.068	0.055	0.028	0.019	0.014
σ	0.995	0.975	0.96	0.938	0.945	0.95	0.972	0.9805	0.986

profiles according to DNS data [58]. The values of the fitting parameters f and σ are presented in Table 1.

As one can see, the dependence of $f(Re)$ is monotonic, while the dependence of $\sigma(Re)$ initially decreases and then increases with increasing Re. Both of these dependencies can be approximated by power functions (see Fig. 12). The following approximation is valid for the parameter f,

$$f = \left(\frac{Re}{1000}\right)^{-3} + 1.155\left(\frac{Re}{1000}\right)^{-0.65}. \qquad (47)$$

For the parameter σ, we have

$$\sigma = 1 + 1.2\left(\frac{Re}{1000}\right)^{-4} - 1.155\left(\frac{Re}{1000}\right)^{-0.65}. \qquad (48)$$

These dependencies make it possible to predict the theoretical velocity profile, as well as estimate the eddy viscosity parameter ν_T and the gradient of angular velocity κ with formulas (45) and (46) using the experimental Reynolds number (Re_{ex}) and half channel width (h_{ex}).

8 Conclusions

Thus, we have considered various types of plane stationary turbulent flows within the framework of a simple model based on the symmetric equations of vortex flow. This model allows for analytical calculations of the mean velocity distribution and includes two main parameters: the turbulence scale (λ), which is determined by the eddy viscosity, and the angular speed of vortex tube rotation (ω). We compared the fitted velocity distributions and experimental profiles for the near-wall flow in a wind tunnel and for Couette and Poiseuille flows in flat rectangular channels. In addition, we compared the model velocity profiles with the results of direct numerical simulations. It is shown that all calculated velocity profiles are in good agreement with the experimental data and the results of the DNS. We believe that the proposed model of plane turbulent flows can be useful for a qualitative consideration of engineering problems in aerodynamics and hydrodynamics.

Acknowledgements
The authors are grateful to Galina Mironova for moral support and to Prof. Yury Stepanyants for fruitful discussions. Special thanks to the reviewers for very useful and stimulating comments.

Authors' contributions
VLM and SVM jointly developed the concept of the vortex model and prepared this manuscript. VLM made the final editing and submitted the manuscript to the editorial office. All authors read and approved the final manuscript.

Funding
Not applicable.

Availability of data and materials
The data and materials used to support the findings of this study are available from the corresponding author upon request.

Declarations

Competing interests
The authors declare that they have no competing interests.

Received: 17 October 2023 Accepted: 24 December 2023
Published online: 13 March 2024

References

1. Gete Z, Evans RL (2003) An experimental investigation of unsteady turbulent-wake/boundary-layer interaction. J Fluids Struct 17(1):43–55
2. Loureiro JBR, Silva Freire AP (2005) Experimental investigation of turbulent boundary layers over steep two-dimensional elevations. J Braz Soc Mech Sci Eng 27(4):329–344
3. Jiménez J (2013) Near-wall turbulence. Phys Fluids 25:101302
4. Reichardt H (1956) Über die Geschwindigkeitsverteilung in einer geradlinigen turbulenten Couetteströmung. Z Angew Math Mech 36(S1):S26–S29. https://doi.org/10.1002/zamm.19560361311
5. Reichardt H (1959) Gesetzmässigkeiten der geradlinigen turbulenten Couetteströmung. Mitteilungen aus dem Max-Planck-Institut für Strömungsforschung und der Aerodynamischen Versuchsanstalt; Nr 22, Göttingen
6. Tillmark N, Alfredsson PH (1992) Experiments on transition in plane Couette flow. J Fluid Mech 235:89–102
7. Bech KH, Tillmark N, Alfredsson PH et al (1995) An investigation of turbulent plane Couette flow at low Reynolds numbers. J Fluid Mech 286:291–325
8. Kitoh O, Nakabyashi K, Nishimura F (2005) Experimental study on mean velocity and turbulence characteristics of plane Couette flow: low-Reynolds-number effects and large longitudinal vortical structure. J Fluid Mech 539:199–227
9. Robertson JM, Johnson HF (1970) Turbulence structure in plane Couette flow. J Eng Mech Div 96(6):1171–1182
10. Huey LJ, Williamson JW (1974) Plane turbulent Couette flow with zero net flow. J Appl Mech 41(4):885–890
11. Laufer J (1951) Investigation of turbulent flow in a two-dimensional channel. NACA Tech Rep NACA-TR-1053
12. Hussain AKMF, Reynolds WC (1975) Measurements in fully developed turbulent channel flow. J Fluids Eng 97(4):568–578
13. El Telbany MMM, Reynolds AJ (1980) Velocity distributions in plane turbulent channel flows. J Fluid Mech 100(1):1–29
14. Ansari S, Rashid MI, Waghmare PR et al (2020) Measurement of the flow behavior index of Newtonian and shear-thinning fluids via analysis of the flow velocity characteristics in a mini-channel. SN Appl Sci 2(11):1787
15. Reynolds O (1895) On the dynamical theory of incompressible viscous fluids and the determination of the criterion. Philos Trans R Soc Lond A 186:123–164
16. McComb WD (1995) Theory of turbulence. Rep Prog Phys 58(10):1117
17 Henry FS, Reynolds AJ (1984) Analytical solution of two gradient-diffusion models applied to turbulent Couette flow. J Fluids Eng 106(2):211–216
18. Hanjalić K, Launder BE (1972) A Reynolds stress model of turbulence and its application to thin shear flows. J Fluid Mech 52(4):609–638
19. Granville PS (1987) Baldwin-Lomax factors for turbulent boundary layers in pressure gradients. AIAA J 25(12):1624–1627
20. Andersson HI, Pettersson BA (1994) Modeling plane turbulent Couette flow. Int J Heat Fluid Flow 15(6):447–455
21. Patel VC, Rodi W, Scheuerer G (1985) Turbulence models for near-wall and low Reynolds number flows: A review. AIAA J 23(9):1308–1319
22. Hanjalić K (1994) Advanced turbulence closure models: a view of current status and future prospects. Int J Heat Fluid Flow 15(3):178–203
23. Launder BE, Spalding DB (1974) The numerical computation of turbulent flows. Comput Methods Appl Mech Eng 3(2):269–289
24. Nagano Y, Tagawa M (1990) An improved k-ε model for boundary layer flows. J Fluids Eng 112(1):33–39
25. Parente A, Gorlé C, van Beeck J et al (2011) Improved k–ε model and wall function formulation for the RANS simulation of ABL flows. J Wind Eng Ind Aerodyn 99(4):267–278
26. Wilcox DC, Traci RM (1976) A complete model of turbulence. In: 9th fluid and plasmadynamics conference, San Diego, 14-16 July 1976
27. Wilcox DC (2008) Formulation of the k-ω turbulence model revisited. AIAA J 46(11):2823–2838
28. Sarkar A, So RMC (1997) A critical evaluation of near-wall two-equation models against direct numerical simulation data. Int J Heat Fluid Flow 18(2):197–208
29. Gerodimos G, So RMC (1997) Near-wall modeling of plane turbulent wall jets. J Fluids Eng 119(2):304–313
30. Spalart PR (1988) Direct simulation of a turbulent boundary layer up to $R_\theta = 1410$. J Fluid Mech 187:61–98
31. Kim J, Moin P, Moser R (1987) Turbulence statistics in fully developed channel flow at low Reynolds Number. J Fluid Mech 177:133–166
32. Abe H, Kawamura H, Matsuo Y (2001) Direct numerical simulation of a fully developed turbulent channel flow with respect to the Reynolds number dependence. J Fluids Eng 123(2):382–393
33. Tsukahara T, Kawamura H, Shingai K (2006) DNS of turbulent Couette flow with emphasis on the large-scale structure in the core region. J Turbul 7(19):1–16
34. Choi YK, Lee JH, Hwang J (2021) Direct numerical simulation of a turbulent plane Couette-Poiseuille flow with zero-mean shear. Int J Heat Fluid Flow 90:108836
35. Guo J, Julien PY (2003) Modified log-wake law for turbulent flow in smooth pipes. J Hydraul Res 41(5):493–501
36. L'vov VS, Pomyalov A, Tiberkevich V (2005) Simple analytical model for entire turbulent boundary layer over flat plane: from viscous and mixing layers to turbulent logarithmic region. Environ Fluid Mech 5:373–386
37. Absi R (2008) Analytical solutions for the modeled k equation. J Appl Mech 75(4):044501
38. Guo J (2018) General mean velocity distribution law for smooth-wall plane Couette flow. J Eng Mech 144(1):04017146

39. Kambe T (2010) A new formulation of equation of compressible fluids by analogy with Maxwell's equations. Fluid Dyn Res 42:055502
40. Marmanis H (1998) Analogy between the Navier–Stokes equations and Maxwell's equations: Application to turbulence. Phys Fluids 10(6):1428–1437
41. Tanışlı M, Demir S, Şahin N (2015) Octonic formulations of Maxwell type fluid equations. J Math Phys 56(9):091701
42. Thompson RJ, Moeller TM (2012) A Maxwell formulation for the equations of a plasma. Phys Plasmas 19:010702
43. Helmholtz H (1858) Über integrale der hydrodynamischen gleichungen, welche den Wirbelbewegungen entsprechen. J Reine Angew Math 1858(55):25–55
44. Mironov VL, Mironov SV (2020) Generalized sedeonic equations of hydrodynamics. Eur Phys J Plus 135(9):708
45. Mironov VL (2021) Self-consistent hydrodynamic two-fluid model of vortex plasma. Phys Fluids 33(3):037116
46. Mironov VL (2022) Self-consistent hydrodynamic model of electron vortex fluid in solids. Fluids 7(10):330
47. Landau LD, Lifshitz EM (1987) Fluid mechanics, 2nd edn. Pergamon Press, London
48. Scheeler MW, van Rees WM, Kedia H et al (2017) Complete measurement of helicity and its dynamics in vortex tubes. Science 357(6350):487–491
49. Boussinesq J (1877) Essai sur la théorie des eaux courante. Imprimerie Nationale, Paris
50. Schmitt FG (2007) About Boussinesq's turbulent viscosity hypothesis: historical remarks and a direct evaluation of its validity. Comptes Rendus Mécanique 335(9–10):617–627
51. Tsukahara T, Kawamura H, Shingai K (2006) DNS database of wall turbulence and heat transfer, Cou3000_A.dat. https://www.rs.tus.ac.jp/t2lab/db/. Accessed 4 Apr 2023
52. Kawamura H, Shingai K, Matsuo Y (2006) DNS database of wall turbulence and heat transfer, Cou12800_A.dat. https://www.rs.tus.ac.jp/t2lab/db/. Accessed 4 Apr 2023
53. Tsukahara T (2007) DNS database of wall turbulence and heat transfer, Poi070_2nd_A.dat. https://www.rs.tus.ac.jp/t2lab/db/. Accessed 20 Aug 2023
54. Kawamura H, Abe H, Matsuo Y (2000) DNS database of wall turbulence and heat transfer, Poi640_2nd_A.dat. https://www.rs.tus.ac.jp/t2lab/db/. Accessed 20 Aug 2023
55. Cess RD (1958) A survey of the literature on heat transfer in turbulent tube flow, Westinghouse Research Laboratory Report 8-0529-R24. Westinghouse Corporation, Philadelphia
56. Symon S, Madhusudanan A, Illingworth SJ et al (2023) Use of eddy viscosity in resolvent analysis of turbulent channel flow. Phys Rev Fluids 8:064601
57. Van Driest ER (1956) On turbulent flow near a wall. J Aeronaut Sci 23(11):1007–1011
58. Kawamura Lab (2007) DNS database of wall turbulence and heat transfer. https://www.rs.tus.ac.jp/t2lab/db/. Accessed 20 Aug 2023